PHYSICAL REVIEW B **75**, 161102(R) (2007)

Coherent vibrations of submicron spherical gold shells in a photonic crystal

D. A. Mazurenko,* X. Shan, J. C. P. Stiefelhagen, C. M. Graf,† A. van Blaaderen, and J. I. Dijkhuis‡
Debye Institute, Department of Physics and Astronomy, University of Utrecht, P. O. Box 80000, 3508 TA Utrecht, The Netherlands
(Received 28 July 2006; revised manuscript received 20 February 2007; published 11 April 2007)

Coherent acoustic radial oscillations of thin spherical gold shells of submicron diameter excited by an ultrashort optical pulse are observed in the form of pronounced modulations of the transient reflectivity on a subnanosecond time scale. Strong acousto-optical coupling in a photonic crystal enhances the modulation of the transient reflectivity by up to 4%. The frequency of these oscillations is demonstrated to be in good agreement with the Lamb theory of free gold shells.

DOI: 10.1103/PhysRevB.75.161102 PACS number(s): 78.47.+p, 42.65.Pc, 42.70.Qs, 63.22.+m

Acoustic motion in nanoscale objects driven by light has attracted considerable attention over the last decade. The interest is explained by various potential applications in nanomechanics, like nanomotors,[1] ultrahigh-frequency acoustic oscillators,[2] and acousto-optic modulators.[3]

Vibrational modes confined in nanoparticles can be excited by a short optical pulse and observed as modulations of the transient reflectivity or transmission on a picosecond time scale.[4] Up to now such vibrations have been observed only in the core of solid particles. Recent progress in fabrication of monodisperse multicoated metallodielectric colloids,[5–7] arranged in a periodic fashion and forming a photonic crystal,[8] makes vibrations localized in thin shells accessible for experiments. Excitation of acoustic vibrations in such structures has two important aspects. First, a shell requires much less vibrational energy than would a massive sphere to reach equal optical responses. Second, the photonic order may enhance the acousto-optic coupling. Thermal quadrupolar hollow-shell vibrations of nickel-silver core-shell nanoparticles have been recently observed in Raman scattering experiments.[9] However, to the best of our knowledge optical excitation of ground-state oscillations localized in a shell has never been shown. In this Rapid Communication we demonstrate optical excitation of coherent radial oscillations of thin gold shells covering inner silica cores of submicrometer diameter. We determine the intrinsic lifetime of these Lamb modes.

Our particles consist of a 228-nm-radius silica core, a gold shell with a thickness of 38 nm, and an outer silica shell with a thickness of 10 nm. The particle size polydispersity is less than 5% as deduced from transmission electron microscopy (TEM) pictures.[8] The particles were assembled in close-packed ordered three-dimensional (3D) arrays, thus forming a metallodielectric photonic crystal that serves to enhance acousto-optical coupling. The details of the particle synthesis can be found in Ref. 8. For our studies we select a highly ordered region on the sample, where the photonic crystal is thicker than the penetration depth of the light, and the reflection from the substrate is negligible. Our structure possesses spatial periodicity for both acoustic and optical properties. Since the spheres are in mechanical contact only at a few points, the acoustic interaction of adjoining spheres is expected to be small and is further neglected. However, the periodic arrangement is important for the electromagnetic waves and here serves to enhance the acousto-optical coupling. The black solid line in Fig. 1 shows a typical linear reflection spectrum of a highly ordered part of our photonic crystal. The spectrum has several resonances, which appear to be much sharper than for a dilute array of the same but in this case optically uncoupled particles.[7] In our sample we distinguish two kinds of resonances.[10,11] First is the so-called Bragg resonance for wavelengths close to the lattice spacing parameter, $\lambda \sim 576$ nm. The spectral position of this resonance is strongly dependent on the incident angle of the incoming light. Second are the collective plasmonic Mie resonances, which are independent of the angle of insidence and dominate the reflection spectrum for $\lambda > 650$ nm. These collective Mie resonances, however, are coupled with Bragg modes, particularly for $\lambda < 650$ nm.

Our sample was excited by a 120-fs pulse extracted from an 800-nm amplified Ti-sapphire laser operating at 1 kHz. The pump pulse was focused onto a 400-μm spot at the sample surface with an energy density of ~ 0.5 mJ/cm^2 per pulse. This density is close to but slightly below the damage threshold and at least one order of magnitude less than the excitation power used to reach the melting temperature in solid spheres.[12] The transient reflectivity was probed by a white-light continuum generated by a beam split off from the same laser and focused either in a cuvette filled with acetone or on a sapphire plate. The white-light pulse was passed via an optical delay line and focused onto a 25-μm spot at the

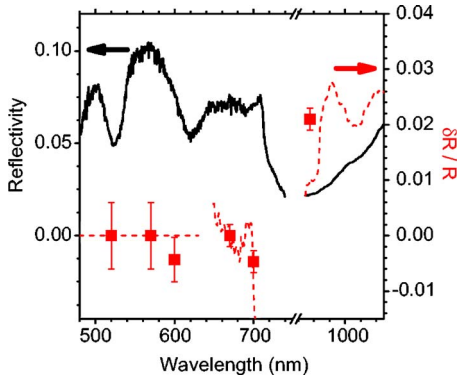

FIG. 1. (Color online) Measured linear reflection spectrum of an ordered 3D array of silica-core gold nanoshells with a silica outer shell (black solid line). Gray (red) squares show the measured amplitude of oscillations in the transient reflectivity, A_1, and dashed line the calculated values $\delta R/R$, according to Eq. (4) for $\lambda > 650$ nm, and $\delta R/R = 0$ for $\lambda < 600$ nm, respectively.

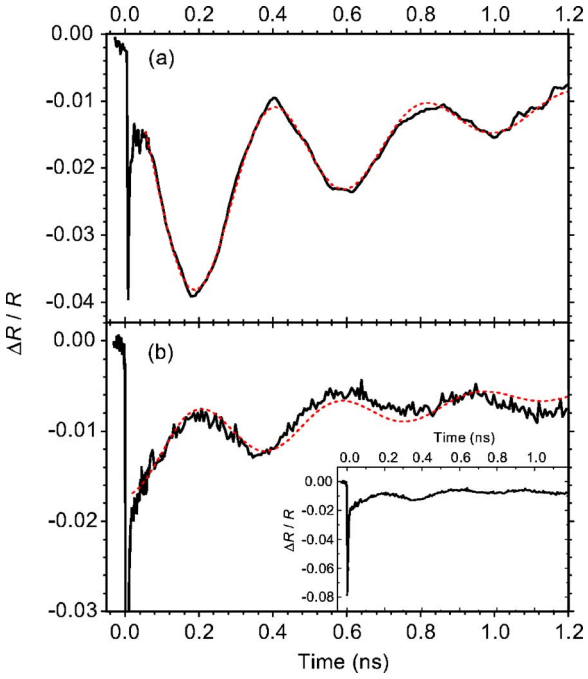

FIG. 2. (Color online) Transient reflectivity dynamics of the gold-shell array measured at (a) 950 and (b) 700 nm. Black solid lines depict experimental data, red dotted lines show the fits. Inset shows the signal measured at 700 nm plotted including the entire electronic contribution.

sample surface within the illuminated area of the pump. The reflected light was subsequently dispersed in a spectrometer and registered by a charge-coupled device (CCD). Temporal evolutions of the reflectivity integrated over a selected 30-nm bandwidth and as a function of delay were detected by an $In_xGa_{1-x}As$ photodetector equipped with an amplifier with 0.1-ms response. The signal from the photodetector was integrated by a digital voltmeter over 10 μs. All experiments have been carried out at room temperature.

The dynamics of the transient reflectivity is found to be dependent on the selected probe wavelength. In Fig. 2, the black solid lines show evolutions of the transient reflectivity $\Delta R/R$ registered at (a) 950 and (b) 700 nm. The inset in Fig. 2(b) shows the signal at 700 nm at full scale. Unfortunately, the spectral range of 740–950 nm was not accessible for measurements because of intense scattering of the 800-nm pump beam. Both curves have a large and sharp peak of picosecond duration immediately after the pump. On a subnanosecond time scale, the transient reflectivity shows a quite distinct behavior. In both Figs. 2(a) and 2(b), we observe pronounced oscillations of the reflectivity with a period of about 400 ps, independent of the probe wavelength λ. The amplitudes of these oscillations, however, are dependent on λ and reach an amplitude as much as 4% of the total reflected intensity at $\lambda=950$ nm [Fig. 2(a)]. In a disordered sample of the same batch of particles, however, we were not able to measure any oscillations. We explain this phenomenon by the fact that optical resonances in our photonic crystal are much sharper than in arrays of individual gold-shell spheres[5–7] and, as a result, exhibit a much stronger acousto-optical coupling. At $\lambda=700$ nm, the amplitude of the oscillations is smaller but still quite sizable. Further, we did observe weak oscillations at 600 nm (not shown in Fig. 2) but we found no oscillations at other wavelengths. It is interesting to note that at 950 and 700 nm the initial peaks have the same signs, while the slow oscillations have opposite polarities. This directly shows that the fast spike and the slow oscillations must have different origins. The temporal evolution of the signal can be approximated quite faithfully by the function

$$\frac{\Delta R}{R} = -A_1 \exp(-t/\tau_1)\cos\left(\frac{2\pi}{T}t-\varphi\right)+A_2\exp(-t/\tau_2). \tag{1}$$

Here, t is time and the fitting parameters T and φ are the period and the phase of the oscillations, respectively, and τ_1 and τ_2 the decay times. Further, A_1 and A_2 are amplitudes referring to the oscillatory and nonoscillatory decay, respectively. The best fits of $\Delta R/R$ for 950 and 700 nm are shown by dotted lines in Figs. 2(a) and 2(b), respectively. The results are collected in Table I. Clearly, the period and the phase of the oscillations are virtually constant over the full spectral range, as are τ_1 and τ_2. The lowest line of Table I collects the average values of all fitting parameters over different wavelengths and points on the sample. We conclude that the detected phase of the oscillations is 0 rad and the period of oscillations is 390 ps with a standard deviation of 5%.

The initial peak in the transient reflectivity is caused by hot electrons in gold. The subsequent dynamics is due to equilibration of the electron gas with the lattice[4] and takes no longer than 20 ps. The nature of the oscillations cannot be found in electron-temperature variations. We attribute the 390-ps oscillations in the transient reflectivity to induced coherent acoustic vibrations of the submicron gold shells following a rapid change in lattice temperature of the gold shell.

In order to determine the eigenfrequencies of the acoustic

TABLE I. Fitting parameters of the transient reflectivity using Eq. (1) for different wavelengths. Last row summarizes the average values from different measurements.

λ (nm)	A_1	A_2	τ_1 (ps)	τ_2 (ps)	T (ps)	φ (rad)
950	−0.021	−0.028	482	1176	406	0.0
700	0.0047	−0.015	633	1510	378	0.08π
600	0.0043	−0.025	770	>1000	381	-0.06π
Average	Depends on λ	Depends on λ	600±200	1300±300	390±20	$0\pm0.1\pi$

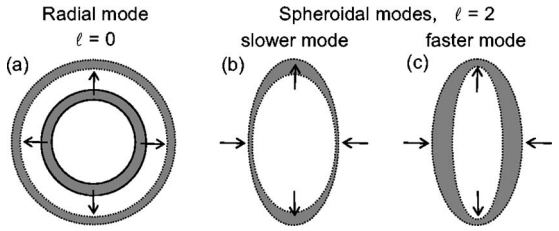

FIG. 3. Sketch of (a) $l=0$ (radial), and (b) and (c) two types of $l=2$ spheroidal vibration modes of a hollow-shell sphere.

vibrations of the particle we assume that the acoustic coupling of the gold shell to the silica core and outer shell is weak and the acoustic response in our particles can be modeled as that of a free-standing thin hollow sphere. This approach is justified by the substantial acoustic mismatch between silica and gold and the weak mechanical contact between core and shell. Indeed, the thermal expansion coefficient is much higher for gold than for silica and, therefore, at elevated temperature the gold shell is not in contact with the silica core. Vibrational modes of a thin shell are classified into two categories—torsional and spheroidal modes,[13] of which only the even-l spheroidal modes are optically active.[14] Of all even-l modes, the most important ones are expected to be the $l=0$ and 2 spheroidal modes because they possess the highest symmetry and therefore optical coupling. A sketch of these modes is presented in Fig. 3.

Assuming zero tension on the interfaces, the period of the Lamb oscillations can be expressed[13] for the ground $l=0$ mode as

$$T_0 = \pi \xi^{-1/2} r_s / c_t, \tag{2}$$

and for the $l=2$ mode as

$$T_{2\pm} = 2\pi [5\xi + 2 \pm (25\xi^2 + 4\xi + 4)^{1/2}]^{-1/2} r_s / c_t. \tag{3}$$

Here, $\xi = 3 - 4(c_t/c_l)^2$, and $c_t = 1200$ m/s and $c_l = 3240$ m/s are the longitudinal and transverse sound velocities of gold, respectively. Further, $r_s = 247$ nm is the average radius of the gold shell. Using Eqs. (2) and (3), we obtain $T_0 = 413$ ps for the $l=0$ mode. The exact solution for a 38-nm-thick shell gives $T_0 = 411$ ps, confirming the validity of the thin-shell approximation. For lower- and higher-frequency branches of $l=2$, we find $T_{2+} = 1074$ ps and $T_{2-} = 249$ ps, respectively. Taking into account a 5% spread in the measured period at different locations on the sample, we arrive at the conclusion that the calculated $l=0$ mode ($T_0 = 411$ ps) is within the experimental error from the value found in the experiment, $T = 390$ ps, while the slower $l=2$ mode is too slow. We also checked that oscillations of the silica core are too fast to explain the experiment: Using the equations for the acoustic vibrations of a solid sphere[15] with $c_t = 3760$ m/s and $c_l = 5970$ m/s for silica, we found a period of 145 ps for the lowest Lamb mode.

Oscillation of the gold shells are the result of the rapid increase of the gold lattice temperature $\Delta\mathcal{T}$ and associated thermal stress induced by hot-electron–phonon relaxation. This is consistent with the observed zero phase of the optical oscillations (see Table I).

Portales *et al.* studied resonant Raman scattering from nickel-silver core-shell particles and found that their spectra can be explained quantitatively by thermal $l=2$ vibrations of the silver shell, i.e., assuming stress-free internal boundary conditions at the core interface.[9] This mode, however, is not observed in our pump-probe experiment. For solid spheres the difference between Raman and pump-probe experiments is well known.[9,16,17] In Raman scattering measurements the excitation is thermal and modes are occupied according to a Planckian distribution. Since Raman scattering is primarily sensitive to dipolar plasmon coupling with the modulation of the surface charges induced by a quadrupole vibration ($l=2$) of the sphere, the $l=2$ peak prevails. In contrast, pump-probe experiments are impulsive, and, after a time much shorter than the period of the acoustic oscillations, electrons are expected to reach a thermal equilibrium distribution in the entire volume, promoting the excitation of the $l=0$ mode. Indeed, the penetration depth of hot electrons in gold is ~300 nm, which is comparable to a quarter of the gold-shell circumference.[18] As a result, the $l=0$ mode is predominantly excited also in our relatively large particles.

The oscillation amplitude of $\Delta R/R$ can be estimated by the following simple model. As already mentioned, the spectral peak near 576 nm is due to Bragg scattering in the photonic lattice. Since the acoustic vibrations of the gold sphere do not affect the lattice parameter of the gold-shell photonic crystal, we expect the oscillation of $\Delta R/R$ to vanish near the Bragg resonance (left red dashed line in Fig. 1). In the red and infrared spectral ranges ($\lambda > 650$ nm), however, the spectral features are due to plasmon resonances. Periodic contractions and dilations of the gold shell lead to a periodic modulation of the dielectric constant of gold, ε, and thus shifts the plasmon resonances back and forth. The modulation of transient reflectivity caused by the acoustic oscillations of shell can be expressed as

$$\frac{\delta R}{R} = \frac{\partial R}{R \partial \lambda} \left(\frac{\partial \varepsilon}{\partial \lambda} \right)^{-1} \delta \varepsilon, \tag{4}$$

where δ denotes the oscillation amplitude. The dielectric constant of gold can be expressed as a sum of the interband and intraband Drude terms, $\varepsilon = \varepsilon^i - \omega_p^2/\omega^2$, with $\omega = 2\pi c/\lambda$ the optical frequency, c the speed of light in vacuum, and ω_p the plasma frequency, which is proportional to the square root of the electron density, $\omega_p \propto \sqrt{n}$. For sufficiently long wavelengths ($\lambda > 650$ nm), we neglect[19] $|\delta\varepsilon^i| \ll |\delta\varepsilon|$, and the modulation of the dielectric constant reads $\delta\varepsilon = -(\omega_p/\omega)^2(\delta n/n)$. Noting that n is inversely proportional to the volume, we obtain $\delta n/n = -3\alpha\Delta\mathcal{T}$, with $\alpha = 1.42 \times 10^{-5}$ K^{-1} the linear thermal expansion coefficient.[20] The rise in the gold temperature, $\Delta\mathcal{T}$, in turn, can be estimated from the electron-phonon equilibration dynamics in the framework of a two-temperature model. Analysis of $\Delta R/R$ kinetics on the picosecond time scale in terms of rapid cooling of the electron gas and heating of the gold lattice[4] allows us to estimate $\Delta\mathcal{T} = 100 \pm 50$ K. In Fig. 1 the middle and right red dashed lines show the estimated $\delta R/R$, which appear to be in qualitative agreement with the experimental data (red solid squares).

The observed decay of the oscillations of $\Delta R/R$ cannot be explained by dephasing caused by inhomogeneous variations in the thickness or diameter of the gold shells. Indeed, the oscillation period of a thin gold shell is independent of the shell thickness. Further, if we assume that the particles are normally distributed with a standard deviation $\sigma_r \ll r_s$, then for $t \ll T r_s/\sigma_r$ the inhomogeneous decay of the oscillation amplitude of $\Delta R/R$ can be expressed as[21]

$$S(t) \propto \cos(2\pi t/T)\exp[-(t/\tau_d)^2], \tag{5}$$

with $\tau_d = r_s T/\sqrt{2}\pi\sigma_r$. Inserting $T=390$ ps and $\sigma_r/r_s=0.05$ known from the TEM data,[8] we obtain $\tau_d=1.75$ ns, which is three times longer than the experimentally observed decay 0.6 ± 0.2 ns. Therefore, this inhomogeneous dephasing mechanism is too slow to fully explain the data. We believe that the decay of oscillations can be explained by residual coupling of the radial $l=0$ mode with other acoustic modes.

In conclusion, the room-temperature transient reflectivity of a photoexcited silica-gold multishell photonic crystal exhibits pronounced oscillations up to the nanosecond time scale. High acousto-optical coupling in our photonic crystal in the red and infrared serves to reach oscillation peak-to-peak amplitude as high as 4% of the total reflectivity at moderate pump power. These oscillations are caused by coherent radial vibrations of the gold shells.[22] The frequency of the acoustic vibrations is found to be in good agreement with classical Lamb theory assuming free boundary conditions on both sides of the shell. The damping of the ground Lamb mode was shown to occur on a subnanosecond time scale and points to a weak interaction with other acoustic modes. Propagation of acoustic waves in a periodic array is an interesting point for future experiments. Of particular interest is the band of acoustic modes between the lowest $l=2$ and the fundamental $l=0$ modes, which is specific for spherical shells. Our result can be useful for various acousto-optical applications, like fabrication of high-frequency band-pass acoustic filters and switching of light propagation in photonic crystals by acoustic waves.

We acknowledge D. B. Murray for his valuable comments on a draft of this paper. We are grateful to C. R. de Kok, P. Jurrius, and P. Vergeer for their technical assistance and A. Meijerink for loaning us the CCD.

*Present address: Zernike Institute for Advanced Materials, University of Groningen, Nijenborgh 4, 9747 AG Groningen, the Netherlands. Electronic address: D.A.Mazurenko@rug.nl

†Present address: Institut für Chemie und Biochemie, Freie Universität Berlin, Takustr. 3, 14195 Berlin, Germany.

‡Electronic address: J.I.Dijkhuis@phys.uu.nl

[1] R. Eelkema, M. M. Pollard, J. Vicario, N. Katsonis, B. S. Ramon, C. W. M. Bastiaansen, D. J. Broer, and B. L. Feringa, Nature (London) **440**, 163 (2006).

[2] X. M. H. Huang, C. A. Zorman, M. Mehregany, and M. L. Roukes, Nature (London) **421**, 496 (2003).

[3] Y. Okawachi, M. S. Bigelow, J. E. Sharping, Z. Zhu, A. Schweinsberg, D. J. Gauthier, R. W. Boyd, and A. L. Gaeta, Phys. Rev. Lett. **94**, 153902 (2005).

[4] For a review, see G. V. Hartland, Annu. Rev. Phys. Chem. **57**, 403 (2006).

[5] R. D. Averitt, D. Sarkar, and N. J. Halas, Phys. Rev. Lett. **78**, 4217 (1997).

[6] S. J. Oldenburg, R. D. Averitt, S. L. Westcott, and N. J. Halas, Chem. Phys. Lett. **288**, 243 (1998).

[7] C. Graf and A. van Blaaderen, Langmuir **18**, 524 (2002).

[8] C. Graf, D. L. J. Vossen, A. Imhof, and A. van Blaaderen, Langmuir **19**, 6693 (2003).

[9] H. Portales, L. Saviot, E. Duval, M. Gaudry, E. Cottancin, M. Pellarin, J. Lermé, and M. Broyer, Phys. Rev. B **65**, 165422 (2002).

[10] D. A. Mazurenko, A. Moroz, C. M. Graf, A. van Blaaderen, and J. I. Dijkhuis, Proc. SPIE **5450**, 569 (2004).

[11] T. A. Kelf, Y. Sugawara, J. J. Baumberg, M. Abdelsalam, and P. N. Bartlett, Phys. Rev. Lett. **95**, 116802 (2005).

[12] A. Plech, V. Kotaidis, S. Grésillon, C. Dahmen, and G. von Plessen, Phys. Rev. B **70**, 195423 (2004).

[13] H. Lamb, Proc. London Math. Soc. **14**, 50 (1882).

[14] E. Duval, Phys. Rev. B **46**, 5795 (1992).

[15] H. Lamb, Proc. London Math. Soc. **13**, 189 (1882).

[16] A. Courty, I. Lisiecki, and M. P. Pileni, J. Chem. Phys. **116**, 8074 (2002).

[17] G. Bachelier and A. Mlayah, Phys. Rev. B **69**, 205408 (2004).

[18] A. A. Maznev, J. Hohlfeld, and J. Güdde, J. Appl. Phys. **82**, 5082 (1997).

[19] M. Garfinkel, J. J. Tiemann, and W. E. Engeler, Phys. Rev. **148**, 695 (1966).

[20] F. C. Nix and D. MacNair, Phys. Rev. **60**, 597 (1941).

[21] G. V. Hartland, J. Chem. Phys. **106**, 8048 (2002).

[22] In a recent paper by C. Guillon, P. Langot, N. Del Fatti, F. Vallée, A. S. Kirakosyan, T. V. Shahbazyan, T. Cardinal, and M. Treguer [Nano Lett. **7**, 138 (2007)], the authors reported on similar acoustic oscillations in disordered Au_2S/Au core-shell particles.